Int J Clin Exp Med 2017;10(5):8438-8448
www.ijcem.com /ISSN:1940-5901/IJCEM0048653

Original Article

Simulated postoperative weight-bearing after fixation of a severe osteoporotic intertrochanteric fracture

Shuang Li[1*], Gui-Xin Sun[2*], Shi-Min Chang[1], Chen-Song Yang[2], Yan Li[3], Wen-Xin Niu[4], Li-Zhi Zhang[1], Chi Zhang[5]

[1]Department of Orthopaedic Surgery, Yangpu Hospital, Tongji University, Shanghai, P. R. China; [2]Department of Traumatology, Shanghai East Hospital, Tongji University, Shanghai, P. R. China; [3]Shanghai University of Sport, Shanghai, P. R. China; [4]Yang Zhi Rehabilitation Hospital, Tongji University, Shanghai, P. R. China; [5]Department of Orthopaedic Surgery, The First Rehabilitation Hospital of Shanghai, Shanghai, P. R. China. [*]Equal contributors.

Received January 11, 2017; Accepted March 2, 2017; Epub May 15, 2017; Published May 30, 2017

Abstract: Unstable intertrochanteric fractures in elderly patients are often associated with a high rate of postoperative complications. The operative procedure used has a great influence on patient outcome, even going so far as to influence mortality rates. Postoperative weight-bearing is also a controversial issue in terms of early rehabilitation and fracture healing. This study uses biomechanical tests and finite element analyses to evaluate the stability of severe osteoporotic intertrochanteric fractures fixed with an Asian proximal femur intramedullary nail antirotation system (PFNA-II). 17 synthetic femoral bones were used for simulating the fracture pattern (AO/OTA type 31-A2) and subsequent fixation. Acetabular loading was manually increased in 100 N increments from 200 N to 1800 N, or until the point of failure. The load applied and number of cycles to failure were recorded and used as inputs to the finite-element analysis. The femur-implant construct had a maximum load to failure of approximately 900 N. The results also revealed the head part had a relative varus displacement to the shaft part. The vertical displacement of the head part is 9.30±0.38 mm (range 9.96-8.91 mm) and transversal displacement is 5.21±0.26 mm (range 5.64-4.91 mm). For securing unstable intertrochanteric fractures, implants are typically designed to substitute as a major weight-bearing structure and to immobilize the fracture. This is particularly important in osteoporosis bone, where the bone is already weakened and susceptible to further damage. This study found that an early weight-bearing load of 900 N (1.45 times body weight) can be recommended for postoperative rehabilitation.

Keywords: Intertrochanteric fracture, finite-element analysis, biomechanical test, proximal femoral nail anti-rotation, PFNA-II, postoperative weight bearing

Introduction

As most healthcare systems across the world try to cope with an aging population, the incidence of osteoporosis and subsequent joint fracture is escalating. 125,000 intertrochanteric fractures are recorded per year in the United States, and this is expected to reach 500,000 by 2040 [1]. As such, intertrochanteric fractures are a worldwide public health issue with devastating consequences for both patients and their families [2, 3]. Invasive intervention (i.e. an operation) is currently the primary, and most successful, method for treating such fractures. However, the choice of procedure and the use of postoperative weight bearing are still controversial. Limited weight bearing reduces mechanical failure, but reduce the patient mobilization [4-6].

The proximal femoral nail anti-rotation (PFNA) system is an intramedullary nail implant designed by the AO/ASIF foundation [7]. As implant designs have improved and demonstrated greater long-term success, such helical blade implants have gradually become more popular and have gained acceptance among trauma surgeons. Nevertheless, implant failure and complications are not uncommon in clinical practice. To avoid the complications, delaying the weight loading or limited weight bearing is the alternative choice for the surgeons and the patients [8].

There is a clear lack of biomechanical and finite element data in the literature to either support or discourage immediate postoperative weight bearing of osteoporotic intertrochanteric fractures. Therefore, the purpose of this investiga-

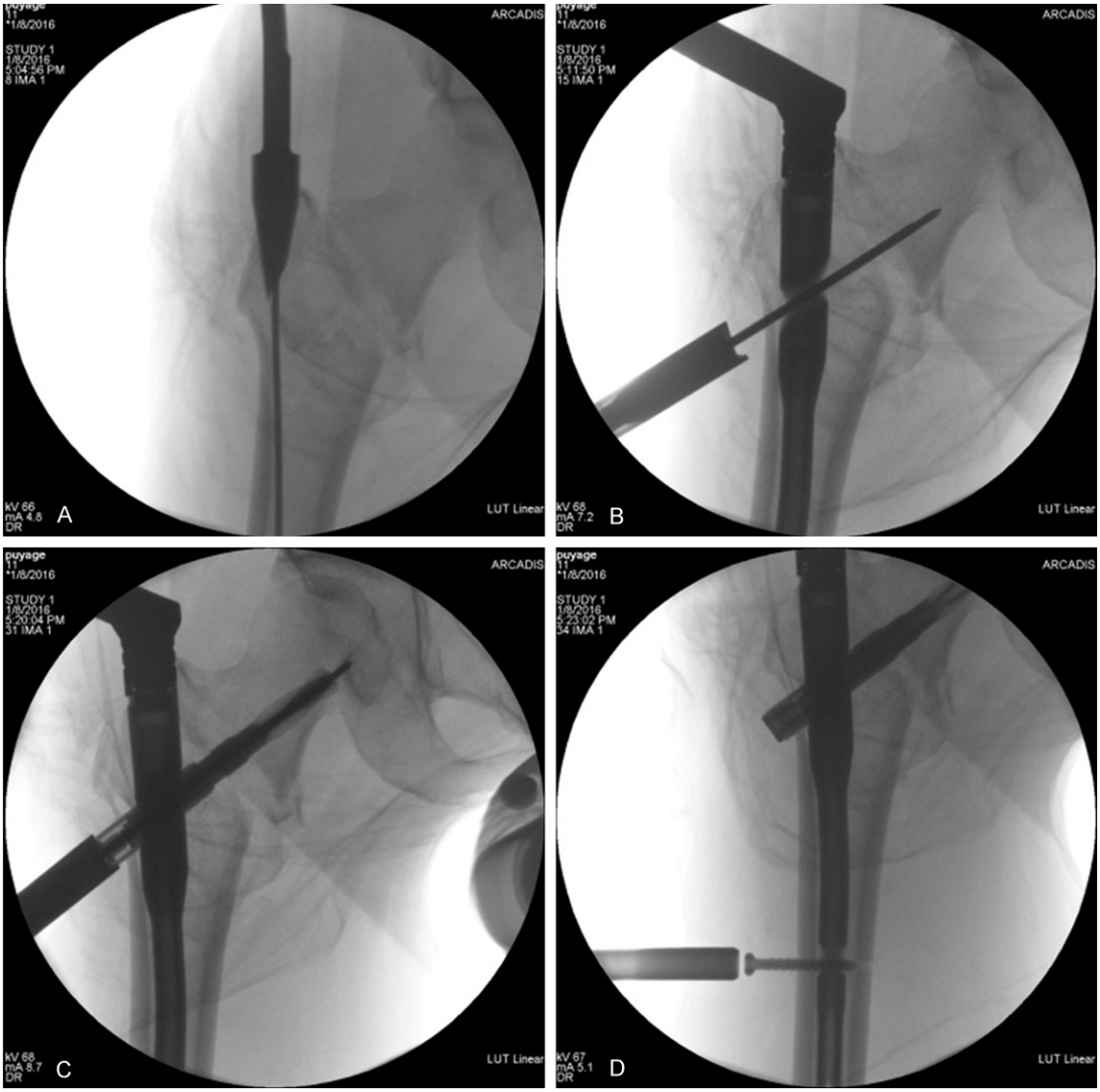

Figure 1. The proximal femur was opened using a conical reamer to gain access to the intertrochanteric fossae (A). The intramedullary nail was then placed into the canal (B). Next, the helical blade is threaded through an opening in the nail and forcibly inserted into the femoral head (C). A distal locking screw holds the blade in place and prevents backward migration (D).

tion is to quantify the effect of immediate weight-bearing on early recovery using in vitro biomechanical tests and finite element analyses.

Materials and methods

General study design

In this study, the PFNA-II system was implanted in synthetic femoral specimens and its performance evaluated using biomechanical tests and numerical analyses. The tests aimed to gauge the stability of fixation and to investigate the short-term behaviors of the osteoporotic fracture fragments. The failure strength of the osteoporotic-femur-implant construct was then used as the applied load in the FEA fatigue analyses to simulate instrumentation of about three months. The numerical results aim to demonstrate the long-term stability and life of the implant-bone construct.

In vitro biomechanical tests

The method is based extensively on those given in parts 3 and 4 of ISO 7206 (ISO 7206-

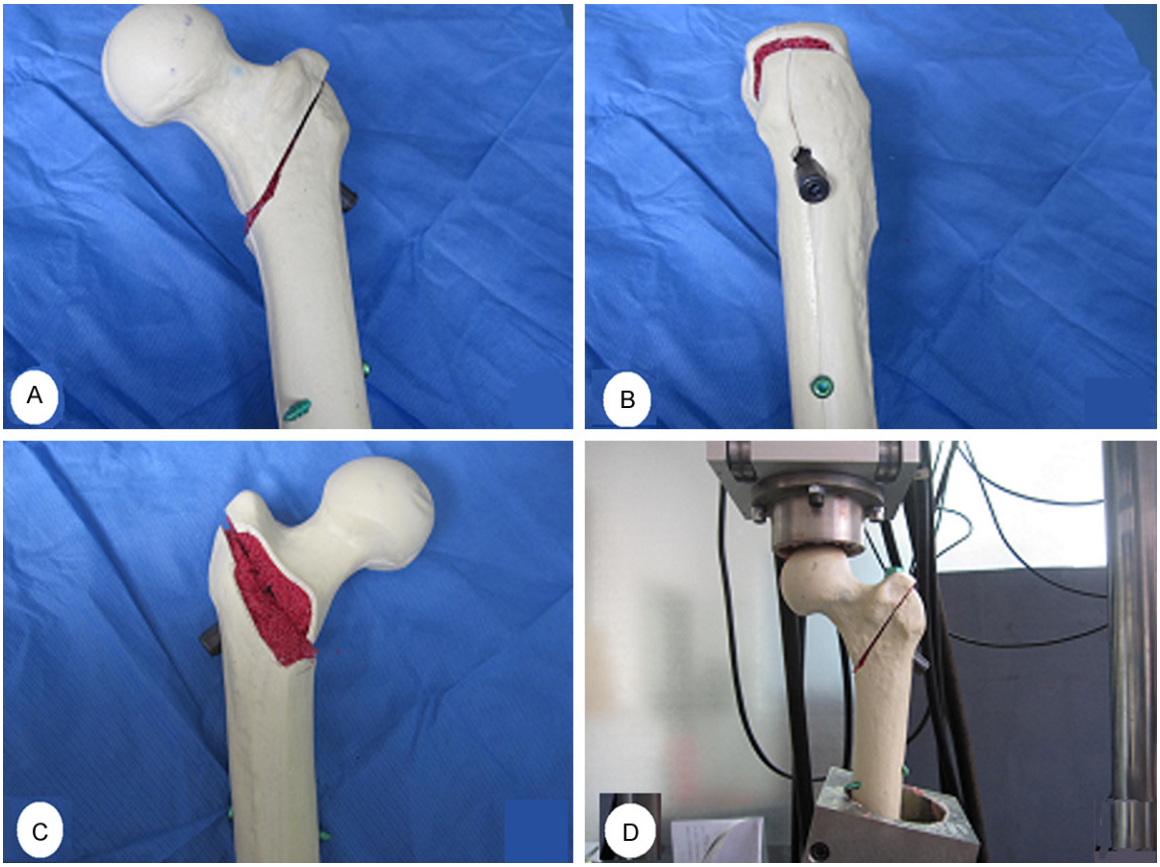

Figure 2. Set up of the MTS system, testing specimens, and fixtures. Specimen implanted with PFNA-II in the frontal plane (A), in the sagittal plane (B) and in the posterior plane (C). Loading study is conducted using a servo hydraulic machine (D).

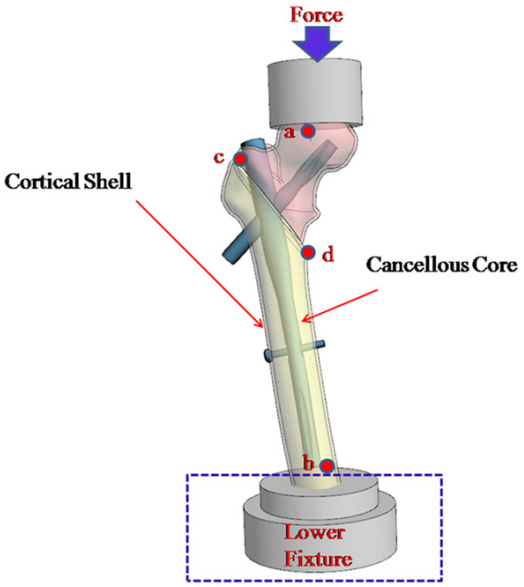

Figure 3. Schematic of the experimental set up of the MTS system. Four points on the femur specimen are shown. Point 'a' is on the femoral head and Point 'b' is on the distal end of the bone. Point 'c' is above the fracture line and Point 'd' is below the fracture line.

6:1992 (E)), which measure the endurance properties of the femur bone and hip joint implant under loading conditions that include a compression of load. The sawbones used in the biomechanical tests were large left fourth-generation composite femurs (model 1130-130, Sawbones AB, Malmo, Sweden). The length from the top of the trochanter to the distal condyle is 45 cm and the cortical walls are 3 mm to 4 mm thick. The density of the open cell cancellous bone is approximately 0.08 g/cm^3 and the cortical bone is 0.32 g/cm^3. The T score was -3.0 so as to simulate a severely osteoporotic bone [9]. The specimens were osteotomized and fixed by a senior orthopedic surgeon using the Asian proximal femur intramedullary nail antirotation system (PFNA-II WG, WEGO ORTHO Corp., China). Intertrochanteric fractures (OTA 31-A2) were recreated by means of osteotomies performed with a guided handsaw and a cutting template [10]. The cutting template assured the reproducibility of the fractures.

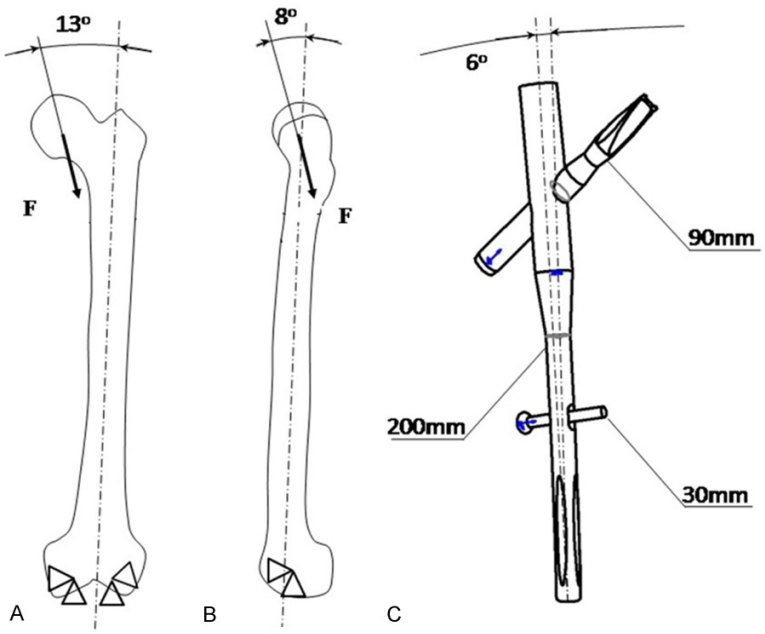

Figure 4. Diagram of the boundary conditions of the FE mode. The vector of the single-stance hip joint force (F) with angles of action in the frontal plane (A) and in the sagittal plane (B). The PFNA implant consists of an intramedullary nail with a proximal angulation of 6° and length 200 mm and a bladed screw with a length of 90 mm (C).

Implantation followed the recommended intramedullary reaming technique for the PFNA-II. The proximal femur was opened using a conical reamer to gain access to the intertrochanteric fossae. The intramedullary nail of length 200 mm was then placed into the canal. Next, the helical blade is threaded through an opening in the nail and forcibly inserted into the femoral head. A distal locking screw holds the blade in place and prevents backward migration. The fracture is reduced so no visible gaps remain between the fragments (**Figure 1A-D**).

The implanted sawbones were mounted into an axial load test jig of a servo hydraulic testing machine (The Shore Western Model 107-160 WhisperPak, Shore Western Manufacturing Inc, USA). Axial loading was applied to the femoral head through a ball-joint-like support (**Figure 2A-D**). The load was manually increased from 200 N to 1800 N in increments of 100 N [10]. 17 composite femurs were performed the fragile biomechanical tests. Each specimen was subjected to sinusoidal loading for 250,000 cycles ranging from the minimum force (200 N) to the maximum force (200 N-1800 N) at a frequency of 4 Hz [11]. Spatial migration of the femoral head test model in relation to the lower fixture was continuously recorded using a pure video-based tracking and analysis software (OptotrakCertus® motion capture system, Canada) (**Figure 3**). Loading was continuously applied a total of 250,000 times and the load-displacement curves were recorded [12]. Before beginning the formal tests, the implanted femurs were held for 4 min at the maximum load to exclude any effects of creep [13]. The load-controlled test machine was programmed to continuously drive the steady movement of the actuator until the femur construct failed. Failure was defined as visible implant mechanical failure (breakage, cut-out and cut through), bone fracture, and fracture mal-reduction.

Finite element analyses

The saw bone models used for biomechanical testing described above were placed in a CT scanner prior to implantation. This allowed reconstruction of complete and identical femur models for finite element analysis. The slice thickness of the CT images was 1.25 mm, with a resolution of 512×512 pixels per image (DICOM format). The DICOM images were imported into Mimics 18.0 software (Materialise N.V., Belgium) to outline the inner and outer contours of the cortical bone. A threshold of 600 Hounsfield units was used to define the boundaries of the cortical shell and cancellous core [14]. The distal end was constrained in all directions in a self-cure denture base material. The angles between the compression force and the bone shaft axis were 13° in adduction in the frontal plane and 8° in the sagittal plane to simulate anatomical loading during single-leg stance [15] (**Figure 4A**, **4B**).

A CAD model of the PFNA-II system was created according to the WEGO ORTHO Corporation' specifications using Solidworks 2014 (Dassault Systems Solid-works Corp., USA). This system

Table 1. Average mechanical properties of bone tissue and implant

	Young's modulus (MPa)	Poisson's ratio
Cortical	17,000	0.3
Trabecular	260	0.3
PFNA-II	110,000	0.33

uses a helical blade with large circumferential contact area for stable fixation (**Figure 4C**). The PFNA models were implanted in the femurs using Abaqus 6.14 (Dassault Systems Solidworks Corp., USA). The Young's modulus was set at 17,000 MPa for cortical bone and 260 MPa for cancellous bone [16]. The PFNA implant was assigned material properties of TiAl6V4, with a Young's modulus of 110,000 MPa and Passion's ratio was set to 0.33 [16] (**Table 1**). All materials were assumed homogeneous, isotropic and linear elastic. Friction coefficients were taken as 0.46 for bone-bone interactions, 0.42 for bone-implant interactions and 0.2 for implant-implant interactions [17] (**Figure 5**). Model convergence was achieved with a cell size of 2.0 mm, whereby the variance ratio of the model stiffness and von Misses stress was less than 2%. The final implant model had 5,455 nodes and 21,711 elements, and the final femoral model had 45,831 nodes and 209,175 elements.

The femur-nail construct was then loaded from 200-1800 N in 100 N increments to calculate the maximum principal stresses. The subsequent fatigue analysis was based on the stress-life method (S-N method). ODB files generated from the Abaqus simulation were then imported into Fe-safe 6.5 (Dassault Systems, Solidworks Corp., USA). 250,000 loading cycles were chosen to simulate instrumentation for three months [17]. The distribution of the equivalent von Mises stress and LOG (Life-Repeats) of the femur and implant were used to predict damage accumulation in the femur over time.

Statistical analysis

Descriptive statistics are used to describe the basic features of the data in the study, and the data was shown as Mean ± SD (n=17). Experimental and numerical data was analyzed using OriginPro 8.5 (OriginLab Corporation, MA, USA) and their coefficients of correlation calculated.

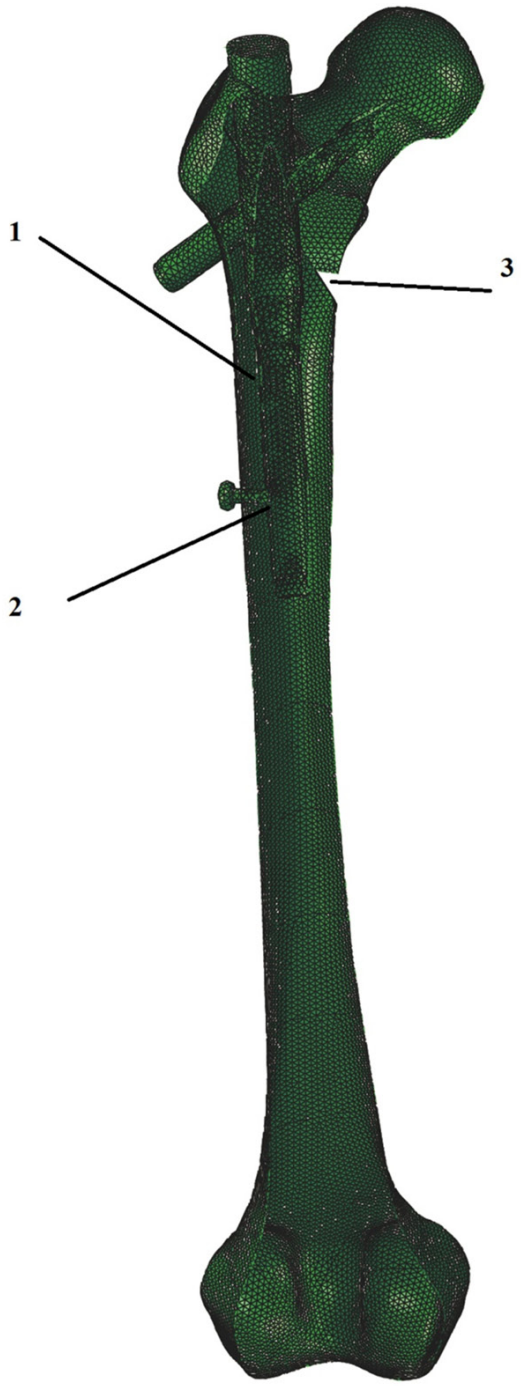

Figure 5. Friction coefficients were taken from literature [17]: 0.42 for bone-implant interactions (1), 0.2 for implant-implant interactions (2), and 0.46 for bone-bone interactions (3).

Results

Biomechanical tests

All experimental displacement results of the femur-implant constructs are shown in **Table 2**.

Table 2. Vertical displacement, transversal displacement and mean loading cycles of the assembly in the *invitro* biomechanical tests

Cyclic load (N)	Vertical Displacement (mm)	Transversal Displacement (mm)	Loading cycles
200~200	8.91	4.91	250000
200~300	8.93	4.95	250000
200~400	8.99	4.97	250000
200~500	9.04	5.12	250000
200~600	9.22	5.23	250000
200~700	9.57	5.34	250000
200~800	9.75	5.53	250000
200~900	9.96	5.64	250000
200~1000	-	-	12204
200~1100	-	-	5
200~1200	-	-	-
200~1300	-	-	-
200~1400	-	-	-
200~1500	-	-	-
200~1600	-	-	-
200~1700	-	-	-
200~1800	-	-	-

No visible nail or screw cracking or cut-out could be seen when placed under loads of up to 900 N. However, the bone failure did occur at 1000 N in the biomechanical tests (**Figure 6A**, **6B**).

For the biomechanical tests, the vertical displacements and transversal displacements of all constructs are listed in **Table 2** and **Figure 7**. Displacement can be seen to increase with increasing loads, with an average final displacement of 9.30±0.38 mm in vertical direction and 5.21±0.26 mm in horizontal, respectively. The mean number of cycles to failure for the specimen loaded to 1000 N was 12,204 cycles, with the specimens (200-900 N) being capable of withstanding greater than 250,000 cycles.

Finite-element analyses

The von Misses stress peaks of the implants and bones are shown in **Figure 8**. The peak von Misses stress of the PFNA-II ranged from 23.479 MPa to 141.931 MPa and the femur ranged from 3.91 MPa to 45.37 MPa, increasing with each subsequent step-up in loading (200-1300 N). Under the 1300 N load, the von Misses stress on the medial region of the intramedullary nail (141.931 MPa) was 98.6% greater than on the lateral region (71.453 MPa).

The construct stiffness is defined as the ratio of the femoral head axial displacement to the applied loads. During validation of construct stiffness, the CAD model was subject to the same loads as in the experimental test. For convergence of displacement, the errors of the numerical and experimental results averaged about 7.8% and their coefficients of correlation were 0.986. The construct stiffness of the finite-element model converged to 1680 N/mm, reaching an element number of about 230,000. Thus the finite-element model was considered validated for further analyses.

The residual life of the femur and cephalo-medullary nails are shown in **Figure 9**, after a simulated three-month implantation period (250,000 loading cycles). The residual life of the construct is only 12,120 cycles under a load of 1000 N. Subjected to dynamic loads from 0 N to 900 N, the residual life of all femur-cephalomedullary-nail constructs tested are similar.

Discussion

The results presented in this study are expressed as the maximum loads borne by the implanted limb. In healthy male individuals, daily activities involving the handling of weight and at the same time temporarily loading only one leg (walking, stair climbing and carrying) generated high hip joint contact forces up to 637%-body weight [18]. As the actual load during the initial three weeks after the operation can range from 60% to 80% body weight, the point at which rehabilitation exercises should be introduced is still controversial [5, 19].

In the severely osteoporotic bone model, the biomechanical tests showed that the mean cycles to implant failure were greater under lower loads than under higher loads. This intact composite bone could withstand pressures as high as 1000 N (60 kg at 1.75 times body weight) [20]. This study found that an early weight-bearing load of 900 N (145%-body weight) can be recommended for postoperative

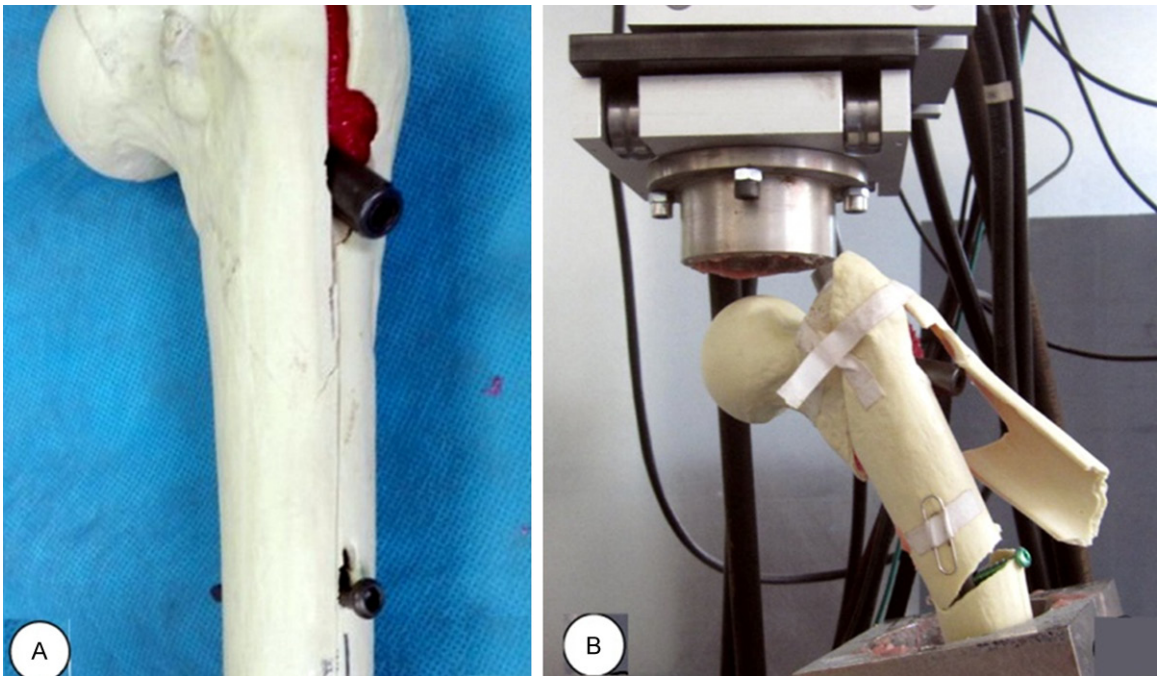

Figure 6. Distalextremity of cortical bone (A) and subsequent rupture of the femoral bone (B).

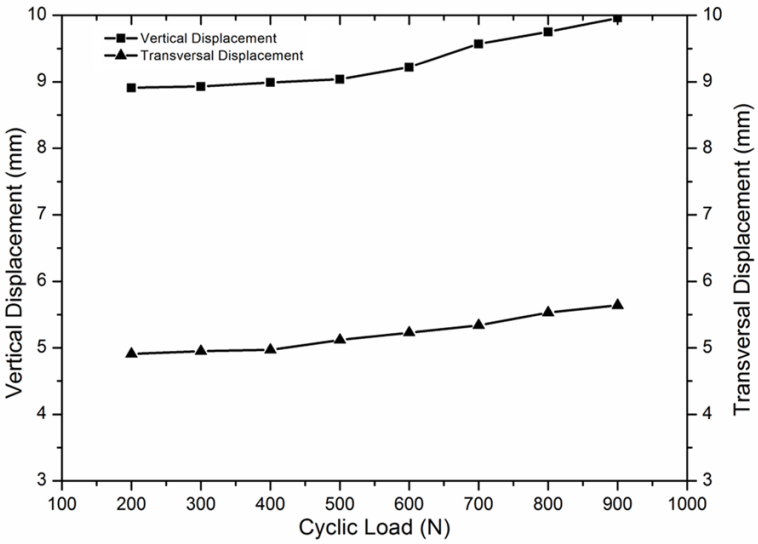

Figure 7. Datum curve of vertical displacement and transversal displacement after cyclic loading.

rehabilitation [21]. The number of loading cycles (250,000+) reported in this study for the blade screw demonstrated its exceptional cut-out resistance [22, 23]. Given the relatively rapid cut-out seen under loads of greater than 1000 N, early-weight bearing should be introduced cautiously and under strict supervision, particularly with overweight patients, so as to reduce the risk of implant failure. In order to control varus mal-reduction and re-fracture, weight-bearing on each leg should be limited to 900 N to prevent bone failure.

This study investigated the effect of stress concentrations, displacement and von Misses stress of a PFNA-II implant under different loads to assess bone and implant stability in a severely osteoporotic intertrochanteric fracture. In general, the implant makes the cortex highly stressed, thus creating a potential source of yielding and cracking around the screw holes (**Figure 6**). As shown in **Figure 8**, the femur is under dual loading in the form of a medial compression force and a lateral tensile force [24]. These forces are then borne by the implant, which provides the majority of the structural support and stability. On average, the screw and nail stresses of the PFNA-II construct were 48.9% higher than those of the femoral bone.

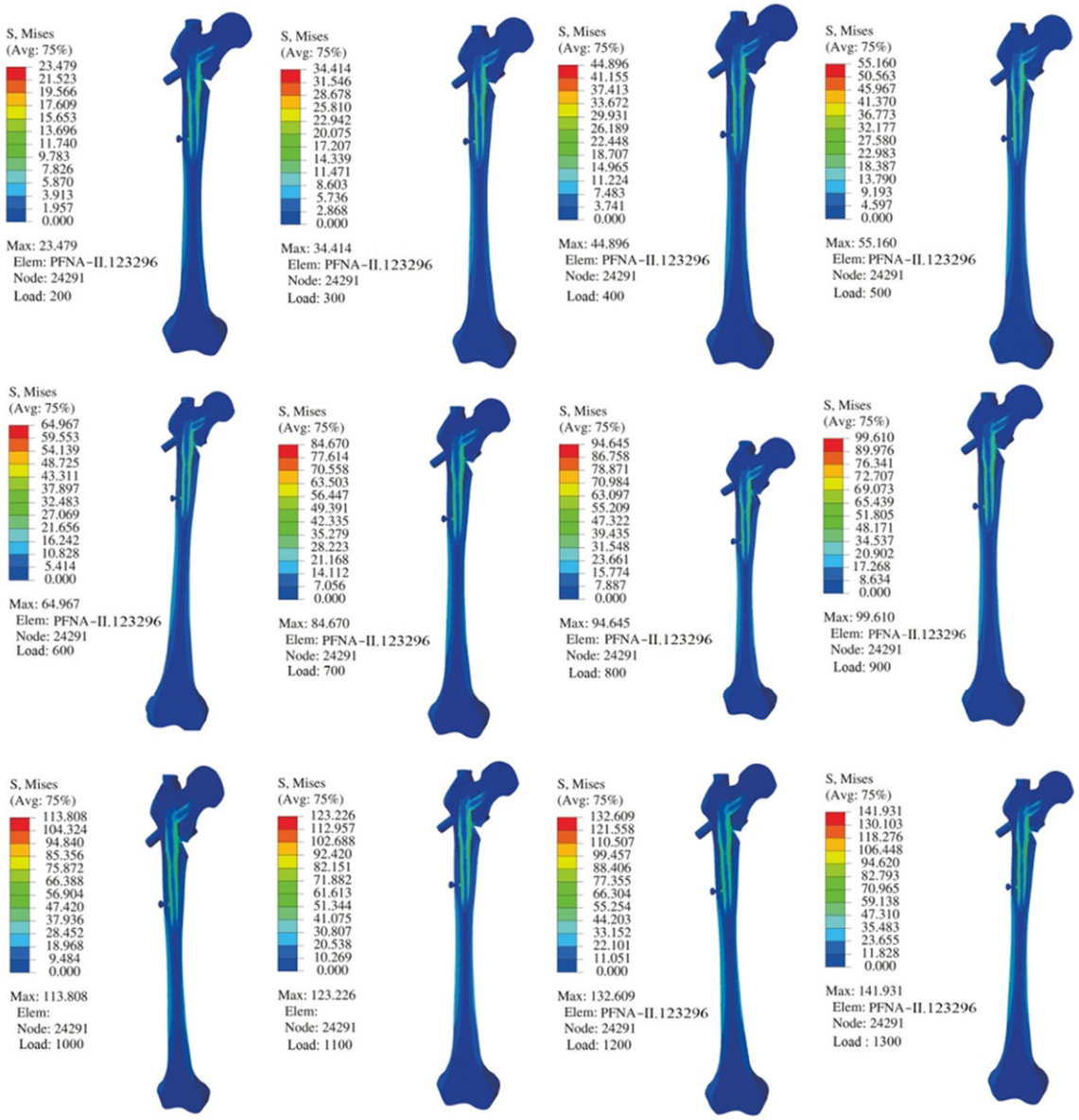

Figure 8. Von Misses stress (MPa) in the bone-implant construct after loading from 200 N-1300 N.

Varus displacement was also observed on the femoral head. Data acquisition is implemented using special markers attached to the bone (**Figure 3**, point a-d). The vertical displacement of the head part is 9.30±0.38 mm (range 9.96-8.91 mm) and transversal displacement is 5.21±0.26 mm (range 5.64-4.91 mm), respectively. This indicates the potential risk of deterioration of the fracture slope, and threatens the residual life of the construct (**Figure 6A**, **6B**). Similar subgroup analyses yielded consistent results for the mean number of cycles to failure loaded to 1000 N (12,204 cycles Vs 12,124 cycles). As noted by Havaldar [25], fracture due to compression in cortical bone depends strongly on the bone tissue volume fraction, the architecture and the mechanical properties of the bone tissue. Failure of the bone-implant construct can be attributed to the weakened strength of the cephalic nail due to varus displacement.

The results of this study suggest that limited weight-bearing immediately after surgery could provide better functional outcomes compared to unrestricted loading when treating intertrochanteric fractures. This is demonstrated by the absence of screw cut-out after 250,000

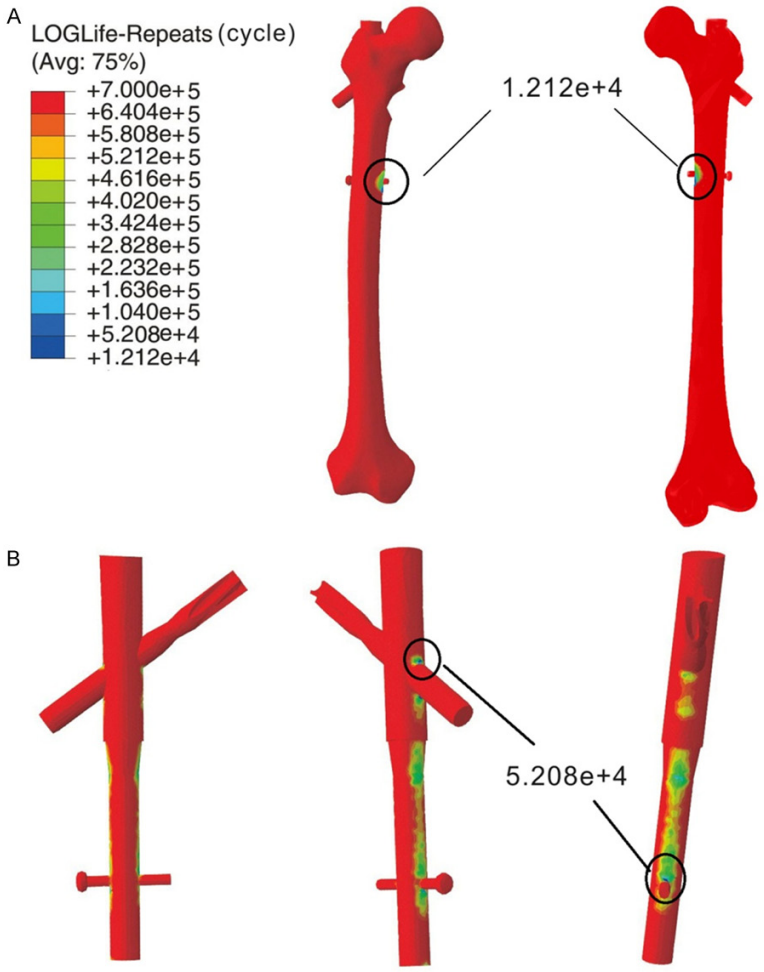

Figure 9. Stress force concentration zone in the femur-implant construct under a load of 1000 N. The fatigue life of the femur is 12,120 cycles and the fatigue life of the PFNA-II implant is 52,080 cycles.

cycles under loads of up to 900 N. However, there are a number of limitations of this study that should be noted. First, the PFNA-II implant was drawn from an image which may not be true to the original dimensions or specifications. The assumption that complete friction and compression force exists between these components may not be fully representative of the true condition. Concerning the boundary conditions, it is believed that this assumption would not affect the findings in this computational analysis. Linear elastic material behavior was also assumed so as to simply the calculation. Second, the implant-bone constructs were examined under one loading and boundary condition based on previous publications without muscle forces [24, 26]. Future developments on this model will include soft tissue forces and more accurately simulate physiological conditions so as to offer a more comprehensive insight into the risk of implant failure and the mechanics between implant-bone interfaces.

In conclusion, this study compares PFNA-II implant displacement and loading cycles under among different loads reflective of weight-bearing post-implantation. The computed results demonstrated that stress concentrations and values increase with more weight-bearing. Furthermore, varus displacement of the implant construct also increased following each increase in loading. The peak von Misses stress for PFNA-II implant was found to lie in the medial and lateral region. This study demonstrates that in elderly patients with an unstable intertrochanteric femoral fracture, a proximal femoral nail provides the majority of the postoperative structural support and stability, but weight-bearing should be limited to 900 N.

Acknowledgements

The authors would like to acknowledge Dr. Jun-Feng Jiang, Dr. Sun-Jun Hu and Ying-Qi Zhang for their help in the methodology. We also thank Dr. Colin McClean for proofreading. The study was supported by fund from Shanghai Municipal Science Committee (No. 14411971900) and the National Natural Science Foundation of China (Grant No. 81572218).

Disclosure of conflict of interest

None.

Address correspondence to: Shi-Min Chang, Department of Orthopedic Surgery, Yangpu Hospital, Tongji University, 450 Tengyue Road, Shanghai 200090, P. R. China. Tel: 8602165690520-608; E-mail: shiminchang11@aliyun.cn

References

[1] Kokoroghiannis C, Aktselis I, Deligeorgis A, Fragkomichalos E, Papadimas D and Pappadas I. Evolving concepts of stability and intramedullary fixation of intertrochanteric fractures-a review. Injury 2012; 43: 686-693.

[2] Volpato S and Guralnik JM. Hip fractures: comprehensive geriatric care and recovery. Lancet 2015; 385: 1594-1595.

[3] Chang SM, Zhang YQ, Ma Z, Li Q, Dargel J and Eysel P. Fracture reduction with positive medial cortical support: a key element in stability reconstruction for the unstable pertrochanteric hip fractures. Arch Orthop Trauma Surg 2015; 135: 811-818.

[4] Zhou JQ and Chang SM. Failure of PFNA: helical blade perforation and tip-apex distance. Injury 2012; 43: 1227-1228.

[5] Koval KJ, Sala DA, Kummer FJ and Zuckerman JD. Postoperative weight-bearing after a fracture of the femoral neck or an intertrochanteric fracture. J Bone Joint Surg Am 1998; 80: 352-356.

[6] Koval KJ, Friend KD, Aharonoff GB and Zukerman JD. Weight bearing after hip fracture: a prospective series of 596 geriatric hip fracture patients. J Orthop Trauma 1996; 10: 526-530.

[7] Simmermacher RK, Ljungqvist J, Bail H, Hockertz T, Vochteloo AJ, Ochs U, Werken Cv; AO - PFNA study group. The new proximal femoral nail antirotation in daily practice: results of a multicentre clinical study. Injury 2008; 39: 932-939.

[8] Augat P, Merk J, Ignatius A, Margevicius K, Bauer G, Rosenbaum D and Claes L. Early, full weightbearing with flexible fixation delays fracture healing. Clin Orthop Relat Res 1996; 194-202.

[9] Cauley JA, Cawthon PM, Peters KE, Cummings SR, Ensrud KE, Bauer DC, Taylor BC, Shikany JM, Hoffman AR, Lane NE, Kado DM, Stefanick ML and Orwoll ES. Risk factors for hip fracture in older men: the osteoporotic fractures in men study (MrOS). J Bone Miner Res 2016; 31: 1810-1819.

[10] Marmor M, Liddle K, Pekmezci M, Buckley J and Matityahu A. The effect of fracture pattern stability on implant loading in OTA type 31-A2 proximal femur fractures. J Orthop Trauma 2013; 27: 683-689.

[11] Luo CA, Hwa SY, Lin SC, Chen CM and Tseng CS. Placement-induced effects on high tibialosteotomized construct-biomechanical tests and finite-element analyses. BMC Musculoskelet Disord 2015; 16: 235.

[12] Windolf M, Braunstein V, Dutoit C and Schwieger K. Is a helical shaped implant a superior alternative to the Dynamic Hip Screw for unstable femoral neck fractures? A biomechanical investigation. Clin Biomech (Bristol, Avon) 2009; 24: 59-64.

[13] Cristofolini L, Affatato S, Erani P, Leardini W, Tigani D and Viceconti M. Long-term implant-bone fixation of the femoral component in total knee replacement. ProcInst Mech Eng H 2008; 222: 319-331.

[14] Tupis TM, Altman GT, Altman DT, Cook HA and Miller MC. Femoral bone strains during antegrade nailing: a comparison of two entry points with identical nails using finite element analysis. Clin Biomech (Bristol, Avon) 2012; 27: 354-359.

[15] Bergmann G, Deuretzbacher G, Heller M, Graichen F, Rohlmann A, Strauss J and Duda GN. Hip contact forces and gait patterns from routine activities. J Biomech 2001; 34: 859-871.

[16] Sitthiseripratip K, Van Oosterwyck H, Vander Sloten J, Mahaisavariya B, Bohez EL, Suwanprateeb J, Van Audekercke R and Oris P. Finite element study of trochanteric gamma nail for trochanteric fracture. Med Eng Phys 2003; 25: 99-106.

[17] Goffin JM, Pankaj P and Simpson AH. The importance of lag screw position for the stabilization of trochanteric fractures with a sliding hip screw: a subject-specific finite element study. J Orthop Res 2013; 31: 596-600.

[18] Varady PA, Glitsch U and Augat P. Loads in the hip joint during physically demanding occupational tasks: a motion analysis study. J Biomech 2015; 48: 3227-3233.

[19] Blaha JD and Logue CM. The biomechanics of hip fractures. Tech Orthop 1989; 4: 7-18.

[20] Do JH, Kim YS, Lee SJ, Jo ML and Han SK. Influence of fragment volume on stability of 3-part intertrochanteric fracture of the femur: a biomechanical study. Eur J Orthop Surg Traumatol 2013; 23: 371-377.

[21] Walpole SC, Prieto-Merino D, Edwards P, Cleland J, Stevens G and Roberts I. The weight of nations: an estimation of adult human biomass. BMC Public Health 2012; 12: 439.

[22] Sommers MB, Roth C, Hall H, Kam BC, Ehmke LW, Krieg JC, Madey SM and Bottlang M. A laboratory model to evaluate cutout resistance of implants for pertrochanteric fracture fixation. J Orthop Trauma 2004; 18: 361-368.

[23] Born CT, Karich B, Bauer C, von Oldenburg G and Augat P. Hip screw migration testing: first results for hip screw and helical blades utilizing a new oscillating test method. J Orthop Res 2011; 29: 760-766.

[24] Samiezadeh S, TavakkoliAvval P, Fawaz Z and Bougherara H. Biomechanical assessment of composite versus metallic intramedullary nailing system in femoral shaft fractures: a finite

element study. Clin Biomech (Bristol, Avon) 2014; 29: 803-810.
[25] Havaldar R, Pilli SC and Putti BB. Insights into the effects of tensile and compressive loadings on human femur bone. Adv Biomed Res 2014; 3: 101.
[26] Filipov O and Gueorguiev B. Unique stability of femoral neck fractures treated with the novel biplane double-supported screw fixation method: a biomechanical cadaver study. Injury 2015; 46: 218-226.